2-2-2 Result of Interpretation

As mentioned in the earlier chapter, the static effects such as the influence of topography and the local resistivity anomaly in the subterranean shallow zone are included in the CSAMT data. In the case of applied one-dimensional interpretation, these influences cannot be evaluated by conducting and the interpreted resistivity structure on the interpreted plane map and interpreted cross section does not correspond to the actual subterranean structure.

Accordingly, this report is applied two-dimensional inversion interpretation to illustrate both the interpreted resistivity plane map and interpreted resistivity cross section for interpreting the resistivity structure in the survey area. The interpreted resistivity cross section is shown in Fig.II-2-7-1 - Fig.II-2-7-13. Also, four different levels of the interpreted resistivity plane maps from the surface to a depth of 50 m, alt.400 m, alt. 300 m and alt.200 m were prepared, which are shown in Fig.II-2-8-1 - Fig.II-2-8-4.

(a) Interpreted resistivity cross section

Almost half of the interpreted resistivity values for all the measurement points are indicated to be between 200 and 500 Ω m. Characteristics that are common to all the measurement points are that a thin layer of the low resistivity below 200 Ω m is distributed in the shallow zone from the surface, and the zone beneath it, the resistivity zone of more than 200 Ω m is distributed. In the area where the high resistivity zones of more than 1000 Ω m in the shallow zone are interpreted, and that the results of some area show the interpreted results that are excessively high comparing with the measured data. Such phenomenon may be resulted from the over fitting, for having the measurement data match better when carrying out the inversion interpretation in which the excessively high resistivity zone appears beneath the thin low resistivity layer in the shallow zone from the surface of the earth.

The following describes the main low and high resistivity zones for each survey line.

On the line A (Fig.II-2-7-1), between the measurement points 100 and 300 from the surface to around alt.200m, the low resistivity zone of below 200 Ω m is distributed. Furthermore, between the measurement points 600 and 1000, from around alt.250m to alt.50m, the low resistivity zone of below 200 Ω m is interpreted. Moreover, the high resistivity zone of more than 1000 Ω m is distributed around the measurement points between 1100 and 1600 from alt.450m to alt.400m, and around the measurement points between 0 and 200, more than a depth of alt.100m.

On the line B (Fig.II-2-7-2) around the measurement points of 200 from alt.300m to 200m, and at the measurement point 500 from alt.300m to 100m, the low resistivity zone of below 200 Ω m is interpreted. Mainly high resistivity zones of more than 1000 Ω m are recognized around the

measurement points from 1600 to 2000, more than a depth of alt.200m, and from the measurement points from 0 to 100, more than a depth of alt.100m. The high resistivity zone is recognized between the measurement points of 600 and 800, 1200 and 1400 and 1900 and 2000 of the shallow sections. However, they can be judged as a results of over fitting.

On the line C (Fig.II-2-7-3), the low resistivity zone of below 200Ωm is interpreted between the measurement points 100 and 400 up to alt.300m from the surface of the earth. Similarly, the high resistivity zone of more than 1000Ωm is distributed between the measurement points 1200 and 1600 from alt.450m to 300m.

On the line D (Fig.II-2-7-4), the low resistivity zone of below 200Ωm is distributed between the measurement points from 0 to 300 up to alt.300m from the surface of the earth.

On the line E (Fig.II-2-7-5), the low resistivity zone of below 200Ωm is distributed between the measurement points 0 and 300 up to alt.300m from the surface of the earth. On the surface of the earth at the measurement points from 600 to 700, the high resistivity zone of more than 1000Ωm is recognized.

On the line F (Fig.II-2-7-6), between the measurement points 0 and 400 from the surface of the earth to around alt.150m, the low resistivity zone of below 200Ωm is distributed. The high resistivity zone of more than 1000Ωm is distributed between the measurement points 600 and 800 from alt.400m to alt.200m.

On the line G (Fig.II-2-7-7), between the measurement points 0 and 400 from the surface to alt.200m, and between the measurement points 1000 and 1200 from alt.250m to alt.50m, the low resistivity zone of below 200Ωm is distributed. Similarly, the high resistivity zone of more than 1000 Ωm is distributed between the measurement points 1300 and 1600 from alt.600m to alt.300m, and between the measurement points 1800 and 2000 from alt.600m to alt.400m.

On the line H (Fig.II-2-7-8), although the low resistivity zone of below 200Ωm is distributed between the measurement points 200 and 400 from alt.300m to alt.100m, it is weak anomaly comparing with that of survey lines from A to G. The high resistivity zone of more than 1000Ωm is distributed between the measurement points 1500 and 2000 from alt.600m to alt.400m.

On the line I (Fig.II-2-7-9), the low resistivity zone of below 200Ωm is distributed between the measurement points 300 and 400 from alt.100m to alt.0m. However, this is weaker anomaly comparing with the line H. The resistivity zone of more 1000Ωm is distributed between the measurement points 600 and 800 from alt.450m to alt.300m, and between the measurement points 1300 and 1500 from alt.500m to alt.350m.

On the line J (Fig.II-2-7-10), the low resistivity zone of below 200Ωm, which lies perpendicular is interpreted between the measurement points 500 and 600 around a depth of alt.50m.

On the line K (Fig.II-2-7-11), the low resistivity zone which lies perpendicular almost same as the

line J is interpreted between the merriment points 500 and 600 from alt.300m to alt.50m. Similarly, the high resistivity zone of more than 1000Ωm is recognized between the measurement points 0 and 500 from alt.450m to alt.200m, between the measurement points 1200 and 1600 from alt.600m to alt.300m and between the measurement points 1700 and 2000 from alt.600m to alt.400m.

On the line L (Fig.II-2-7-12), the low resistivity zone of below 200Ωm is not distributed, but the high resistivity zone more than 1000Ωm is distributed in the wide range of area between the measurement points 100 and 500 from alt.500m to alt.200m, between the measurement points 800 and 1600 from alt.700m to alt.-100m and also between the measurement points 1800 and 2000 from alt.500m to alt.400m.

On the line M (Fig.II-2-7-13), the low resistivity zone of below 200Ωm is not distributed the same as line L, but the high resistivity zone of more than 1000Ωm is distributed between the measurement points 100 and 600 from alt.500m to alt.200m. Similarly, the high resistivity zone of more than 1000Ωm is distributed in the band area between the measurement points 700 and 2000 from alt.600 and alt.-100m.

(b) Interpreted resistivity plane map

The interpreted resistivity plane map of a depth of 50m from the surface of the earth is shown in Fig.II-2-8-1. The average interpreted resistivity value is 534.3Ωm (minimum 43.6Ωm, maximum 3380.9Ωm). The low resistivity zone with less then 200Ωm is distributed in the wide range of area, which crosses the survey lines almost perpendicularly in the direction of NE-SW as follows: on the line C at the measurement point 200, on the line D between the measurement points 100 and 200, on the line E between the measurement points 0 and 300, and on the line F between the measurement points 300 and 0. Also, it is locally distributed on the line C at the measurement point 1000 and on the line D at the measurement point 1100.

The interpreted resistivity plane map of alt.400m is shown in Fig.II-2-8-2. The average interpreted resistivity value is 525.0Ωm (minimum 17.6Ωm, maximum 2817.5Ωm). The low resistivity zone of less then 200Ωm is distributed in the south east of survey area, which crosses the survey lines almost perpendicularly in the direction of NE-SW as follows: on the line C at the measurement point 200, on the line D between the measurement points 100 and 200, on the line E between the measurement points 0 and 300, and on the line F between the measurement points 0 and 300, on the profile G between the measurement points 100 and 300, oh the line H between the measurement points 0 and 300 and on the line I at the measurement point 0. Also, the low resistivity zone is separately distributed from the line H at the measurement point 300 and to the line J at the measurement point 600. These resistivity zones connecting in the direction of N-S are assumed.

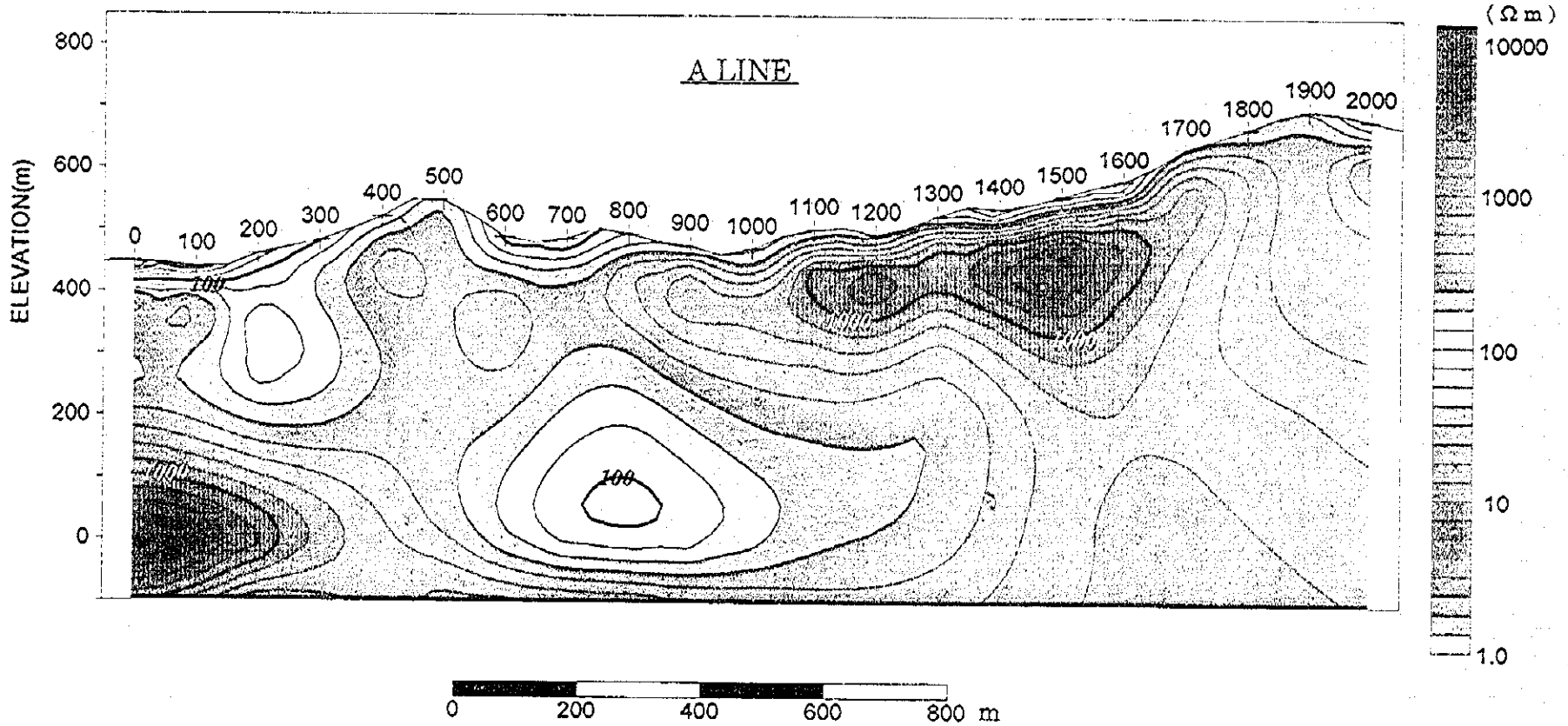

Fig.II-2-7.1 Interpreted resistivity cross section for A line

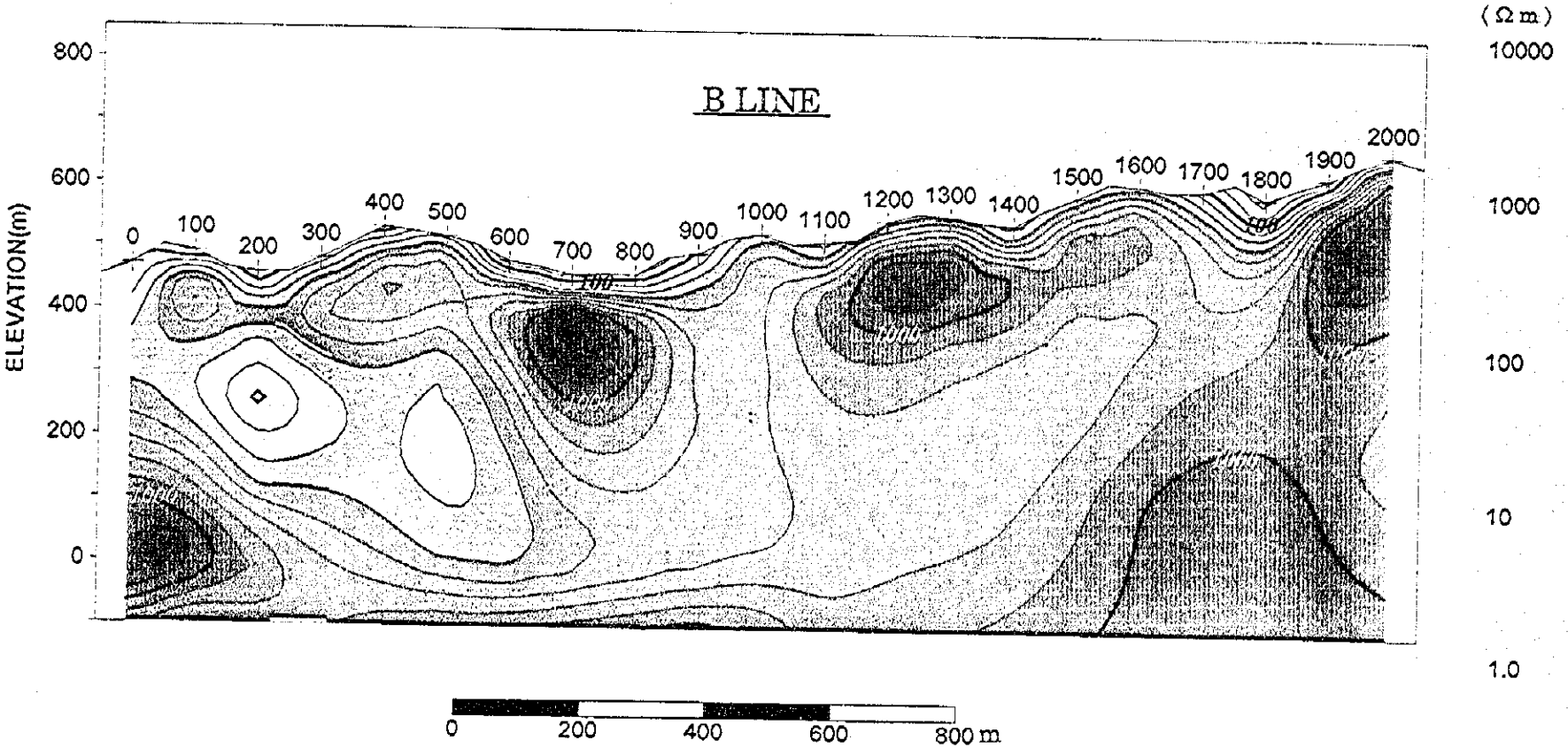

Fig.II-2-7.2 Interpreted resistivity cross section for B line

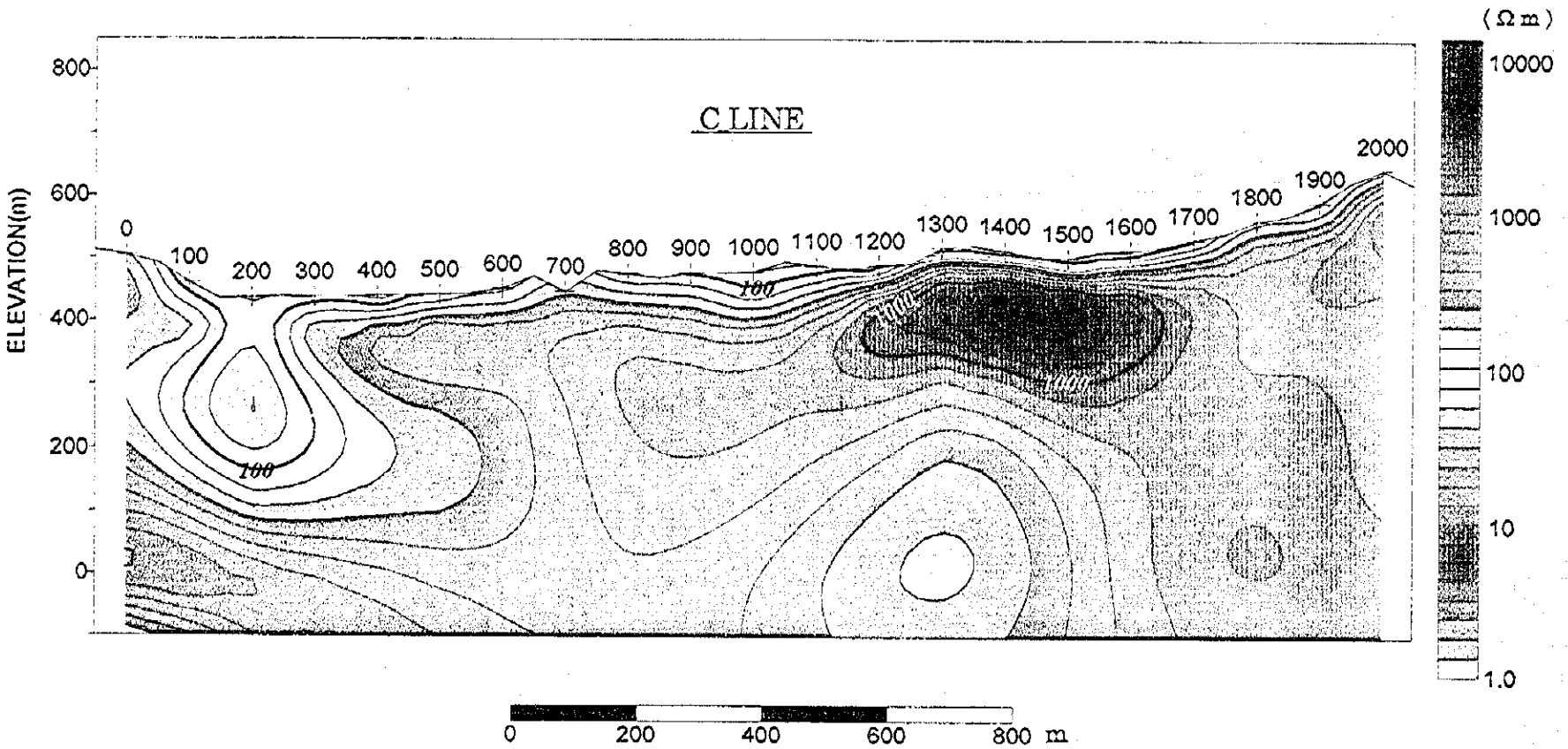

Fig.II-2-7.3 Interpreted resistivity cross section for C line

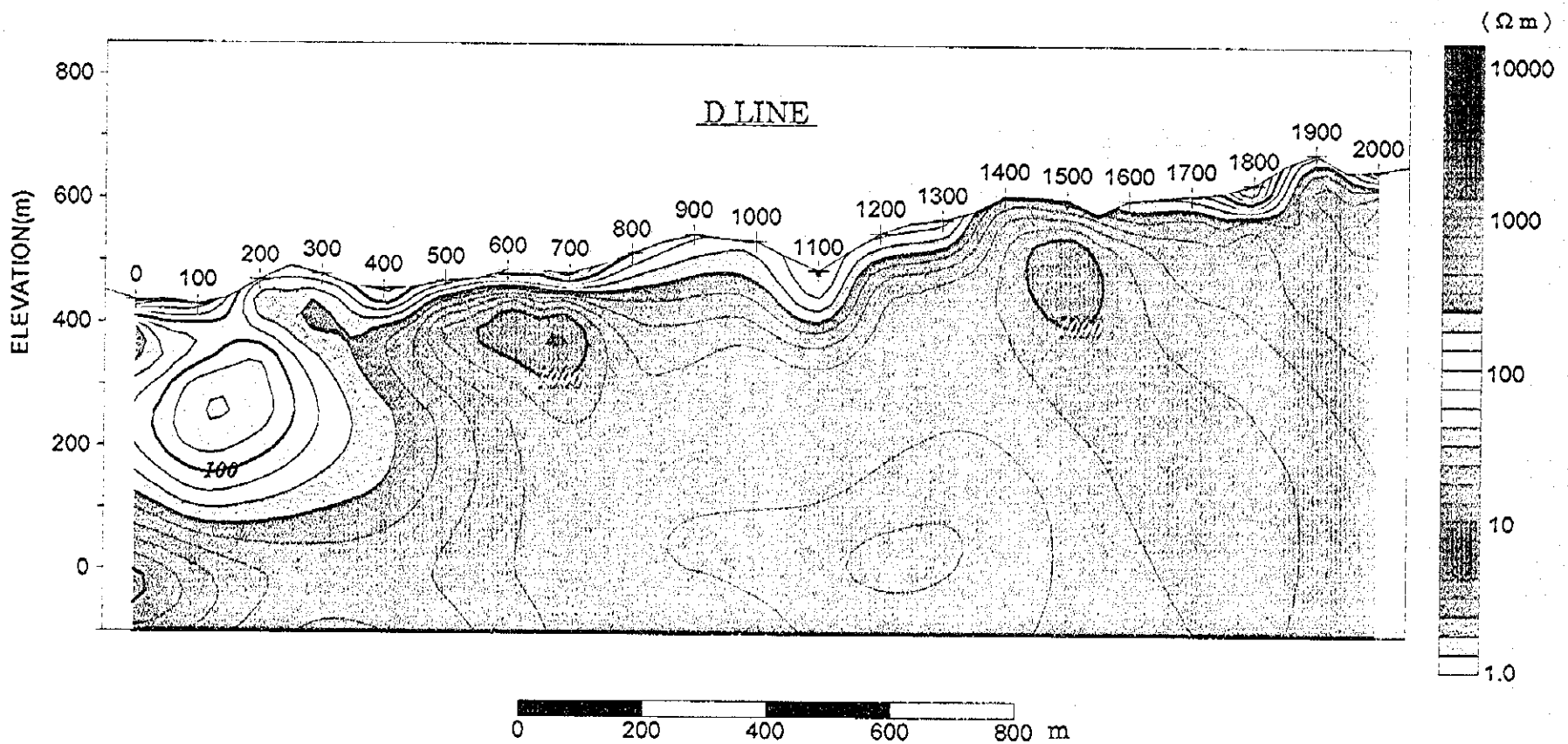

Fig.II-2-7.4 Interpreted resistivity cross section for D line

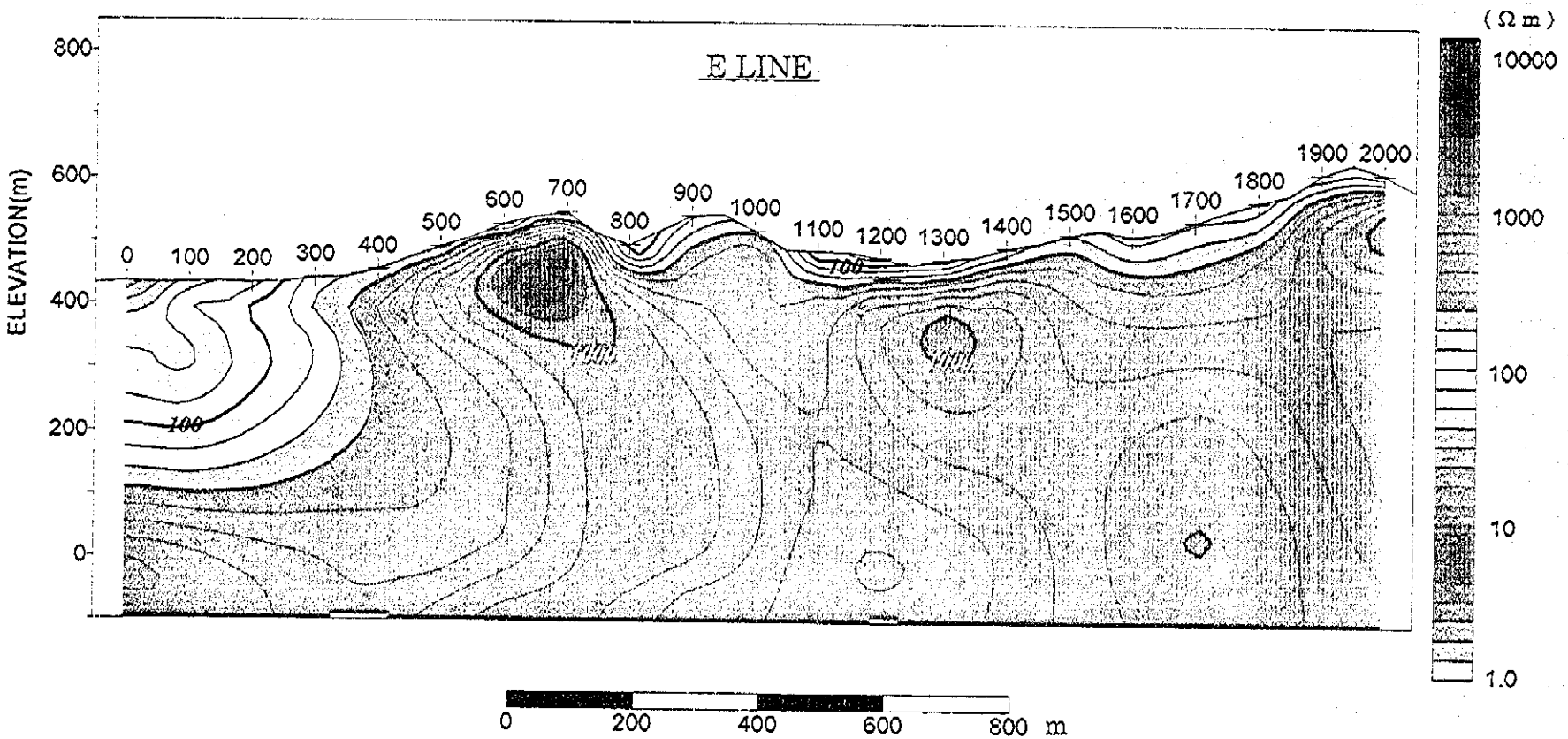

Fig.II-2-7.5 Interpreted resistivity cross section for E line

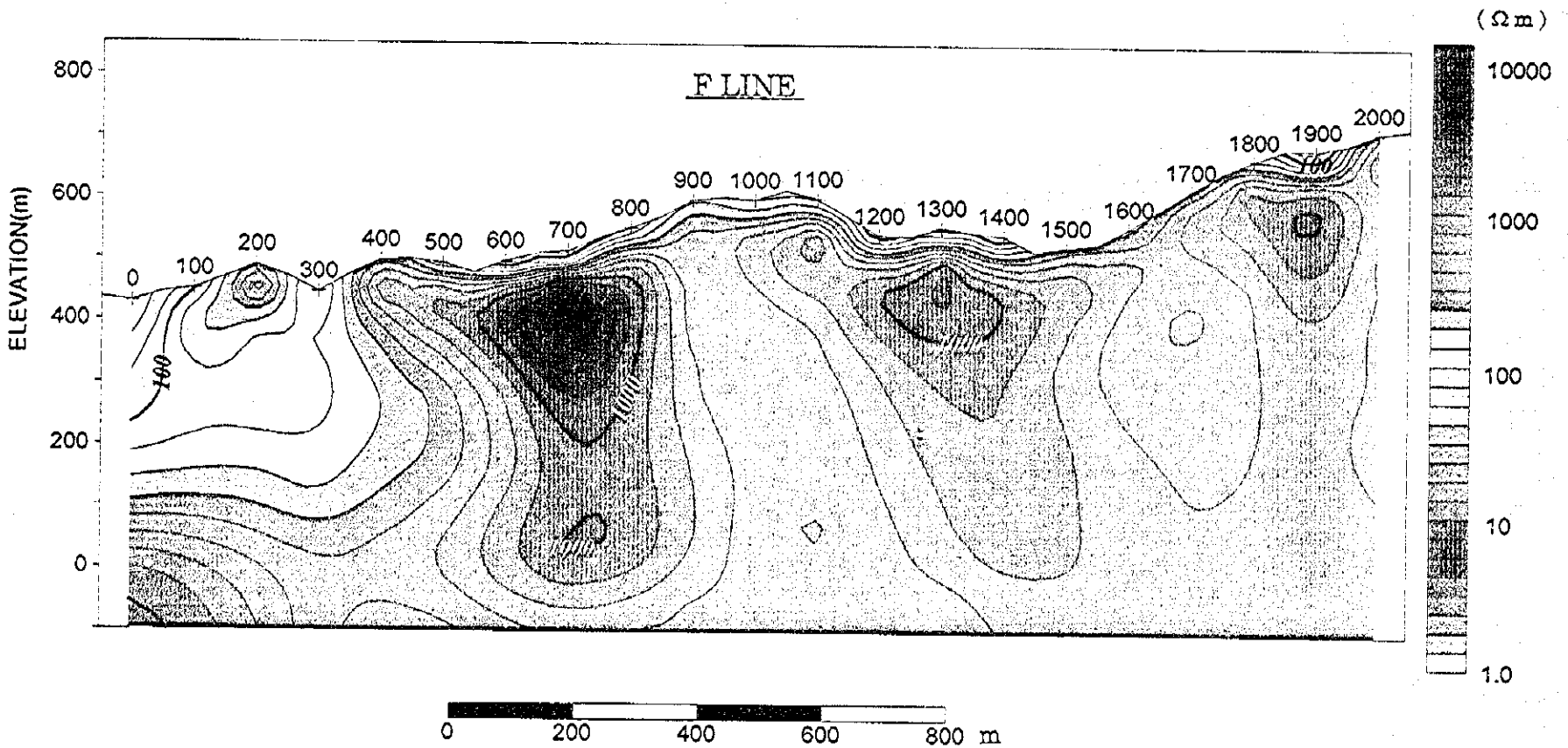

Fig.II-2-7.6 Interpreted resistivity cross section for F line

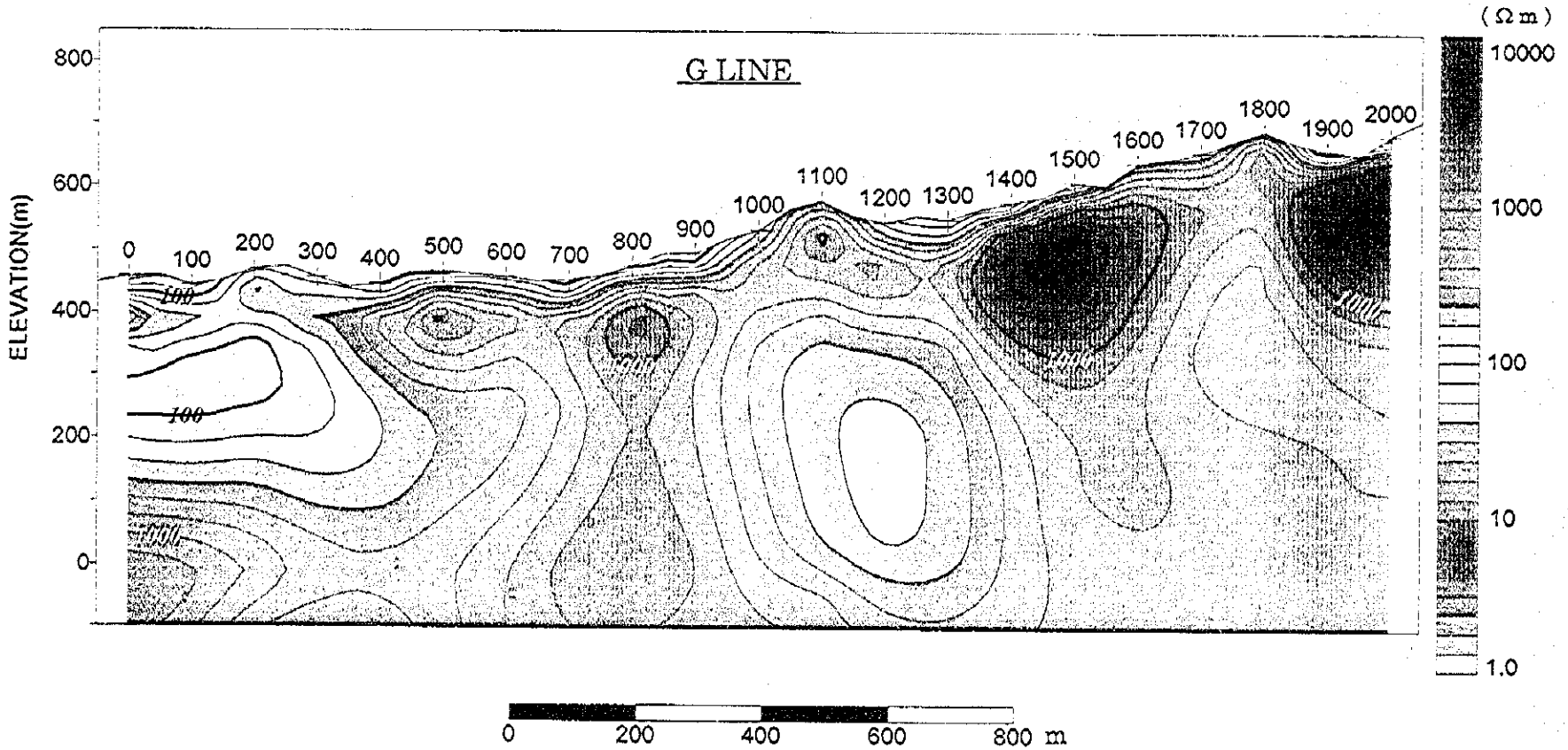

Fig.II-2-7.7 Interpreted resistivity cross section for G line

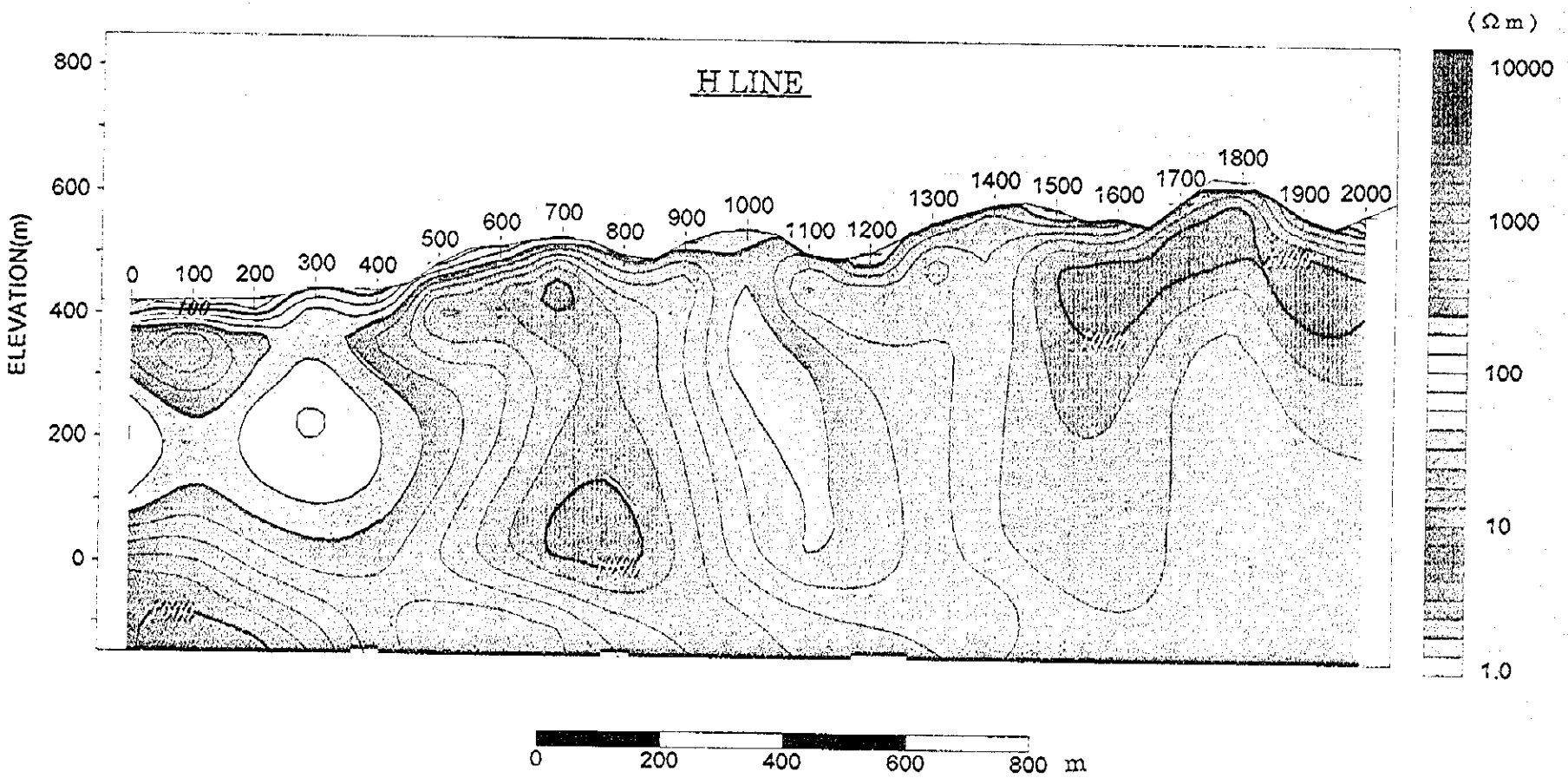

Fig.II-2-7.8 Interpreted resistivity cross section for H line

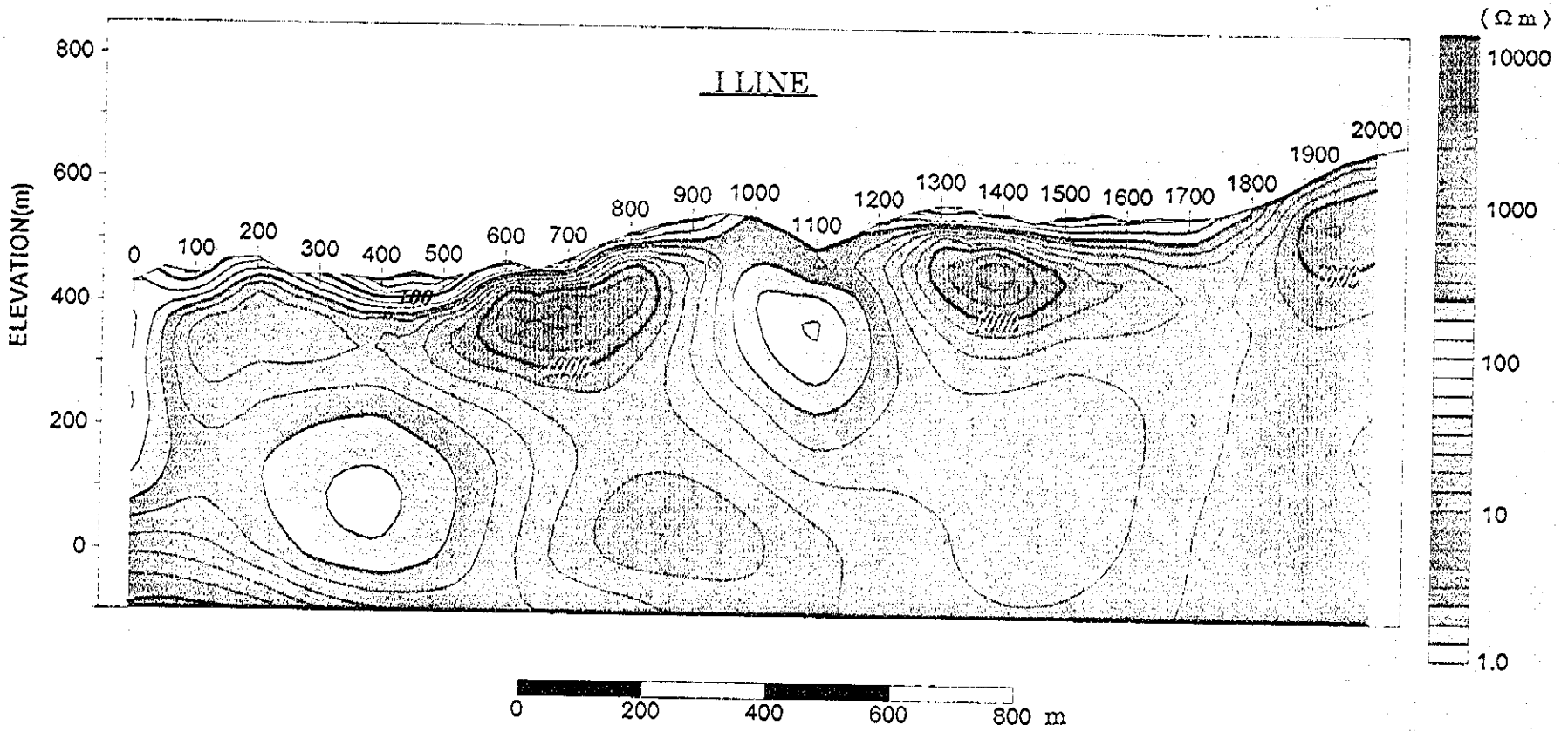

Fig.II-2-7.9 Interpreted resistivity cross section for I line

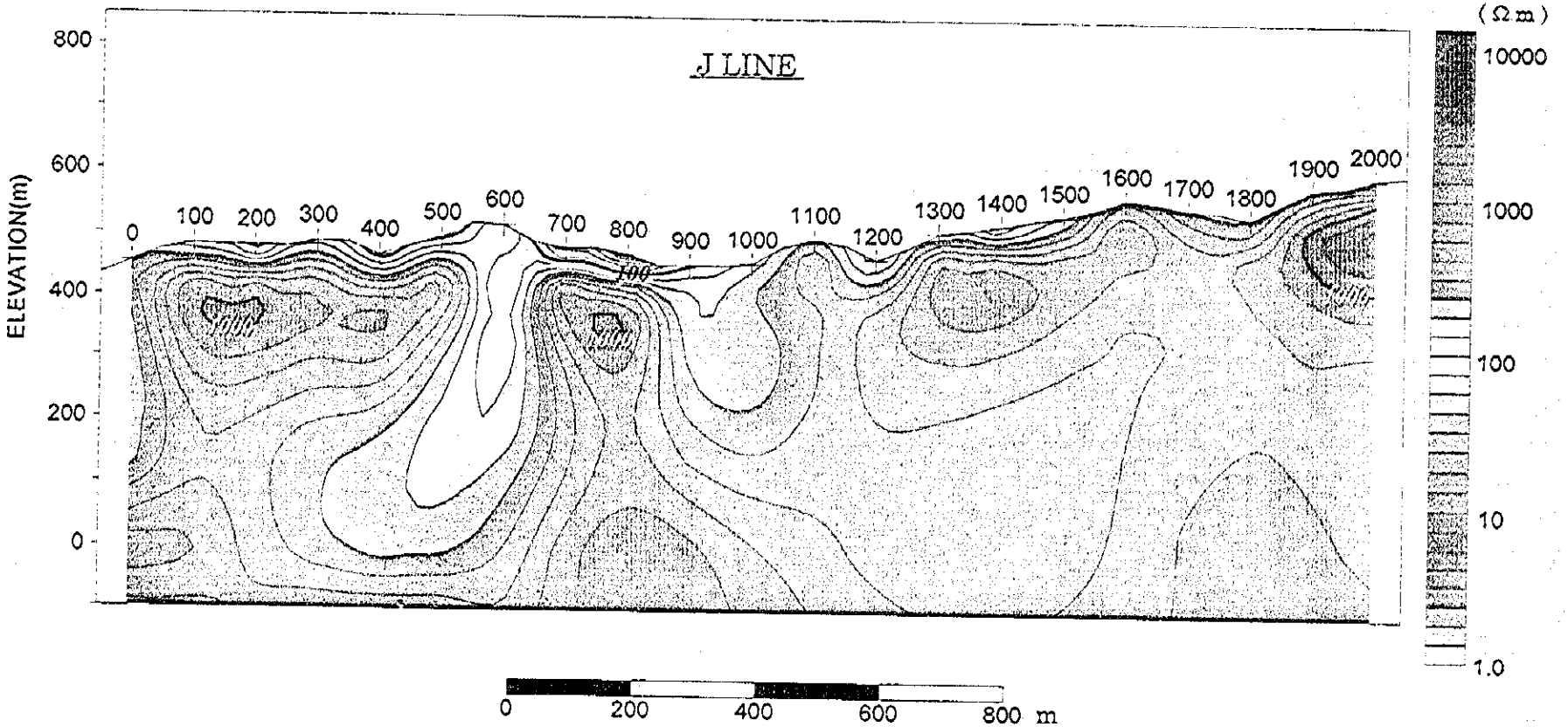

Fig.II-2-7.10 Interpreted resistivity cross section for J line

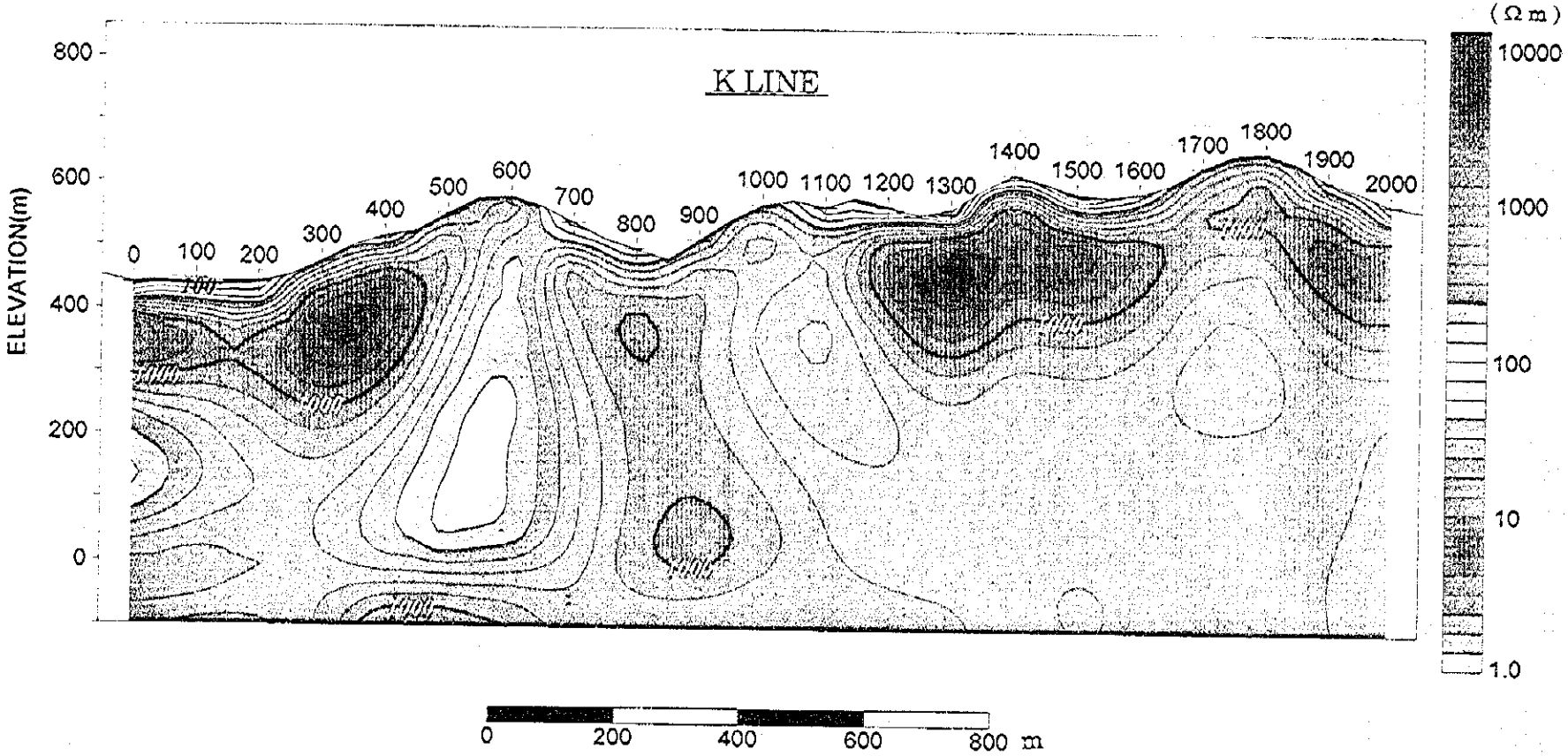

Fig.II-2-7.11 Interpreted resistivity cross section for K line

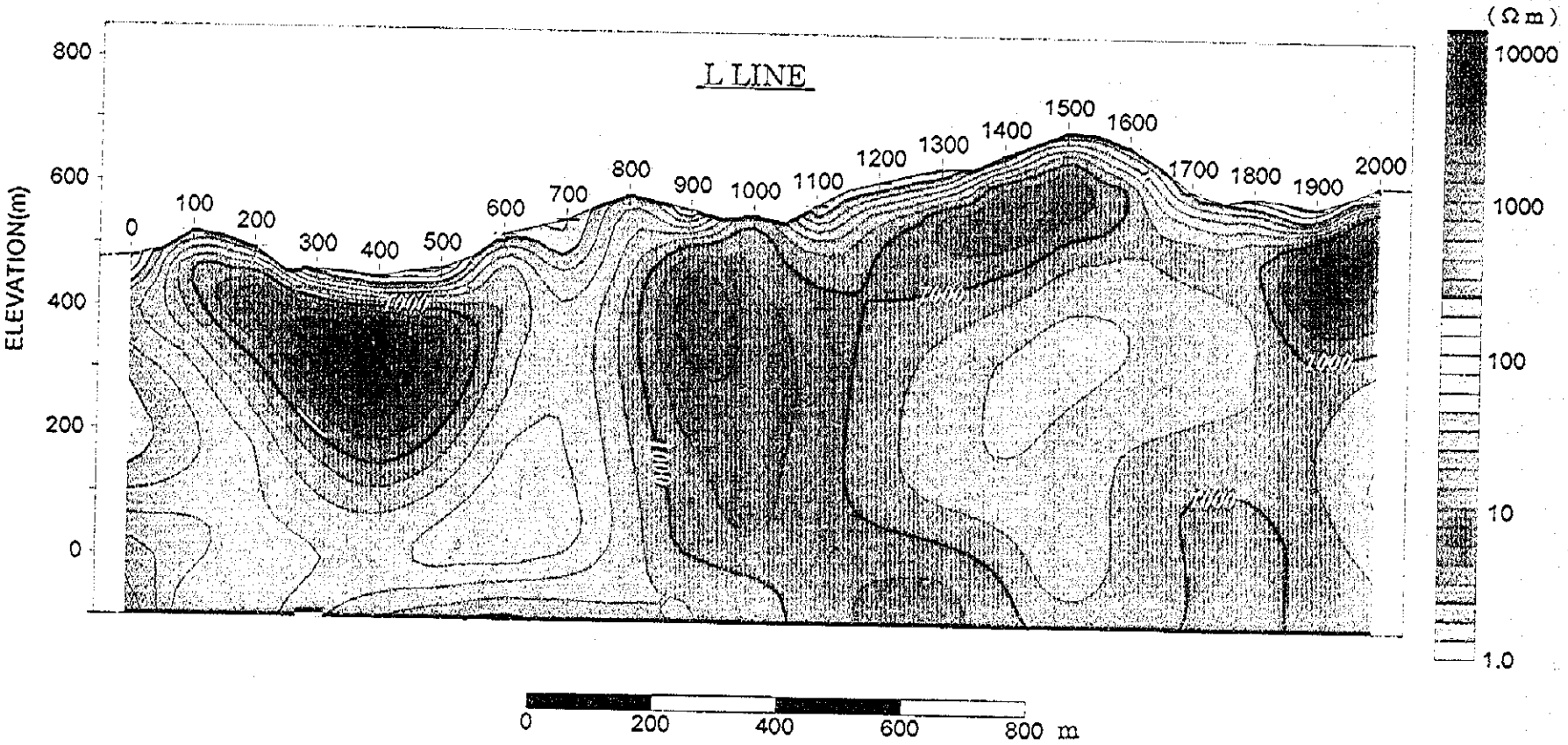

Fig.II-2-7.12 Interpreted resistivity cross section for L line

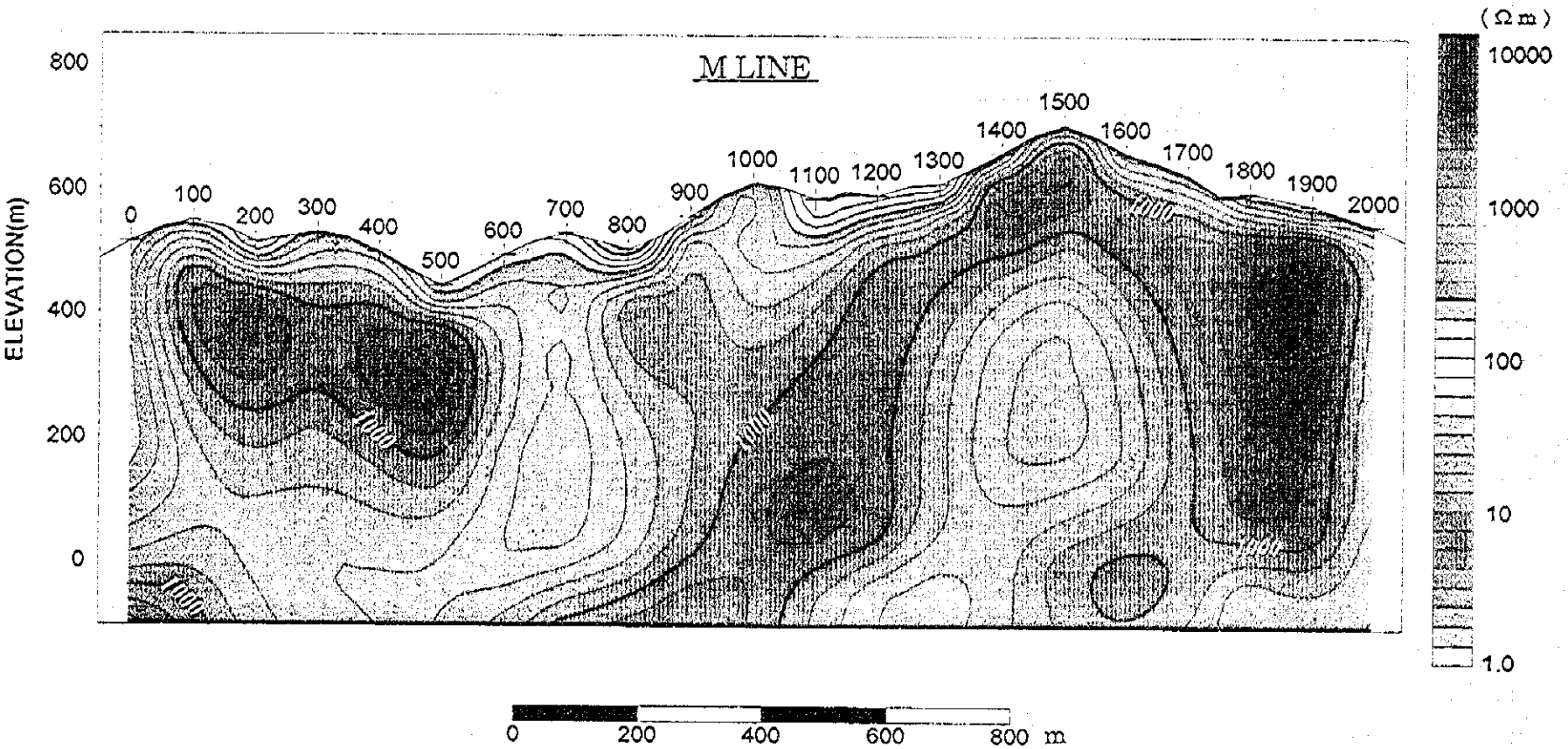

Fig.II-2-7.13 Interpreted resistivity cross section for M line

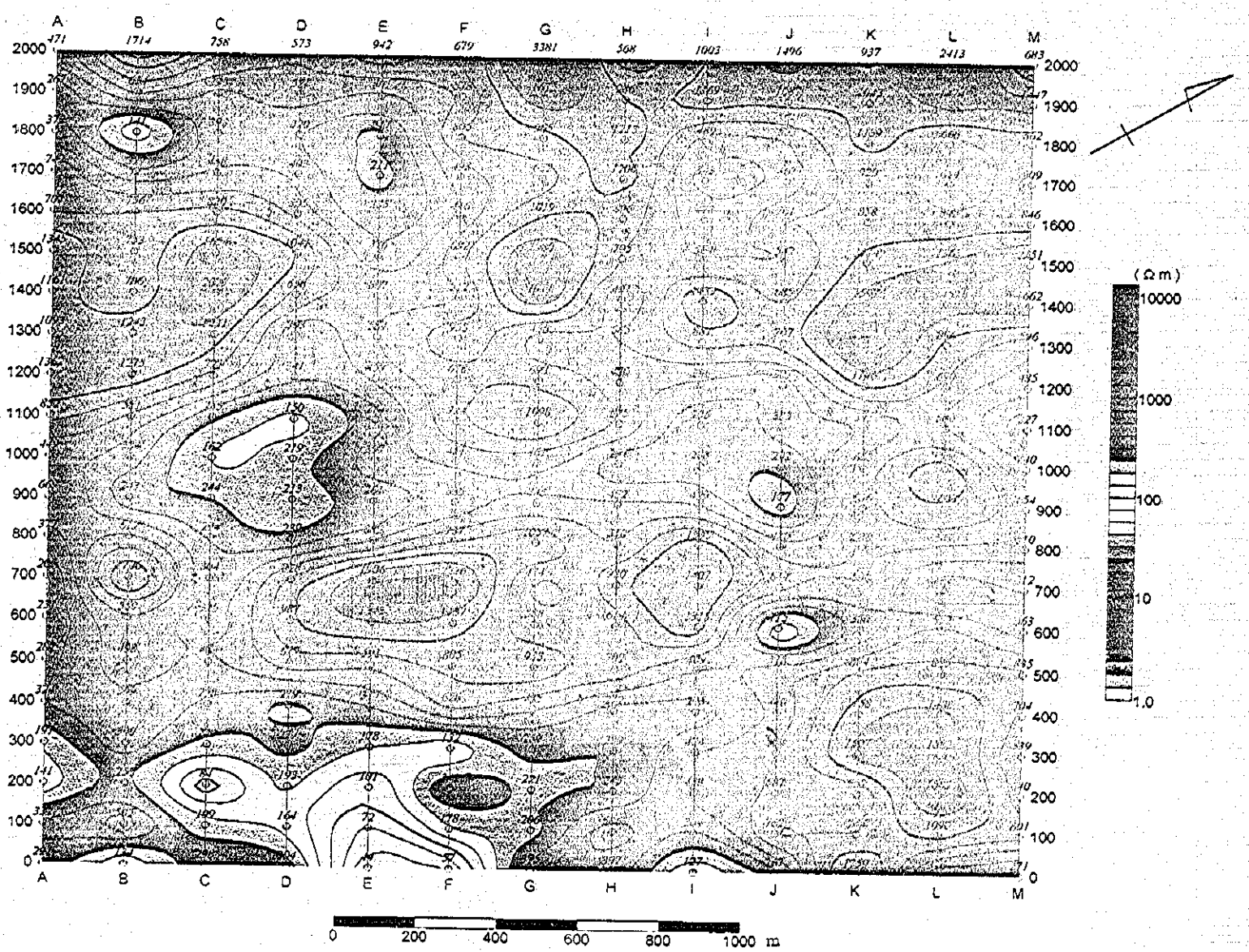

Fig.II-2-8.1 Interpreted resistivity plan map for G.L -50m

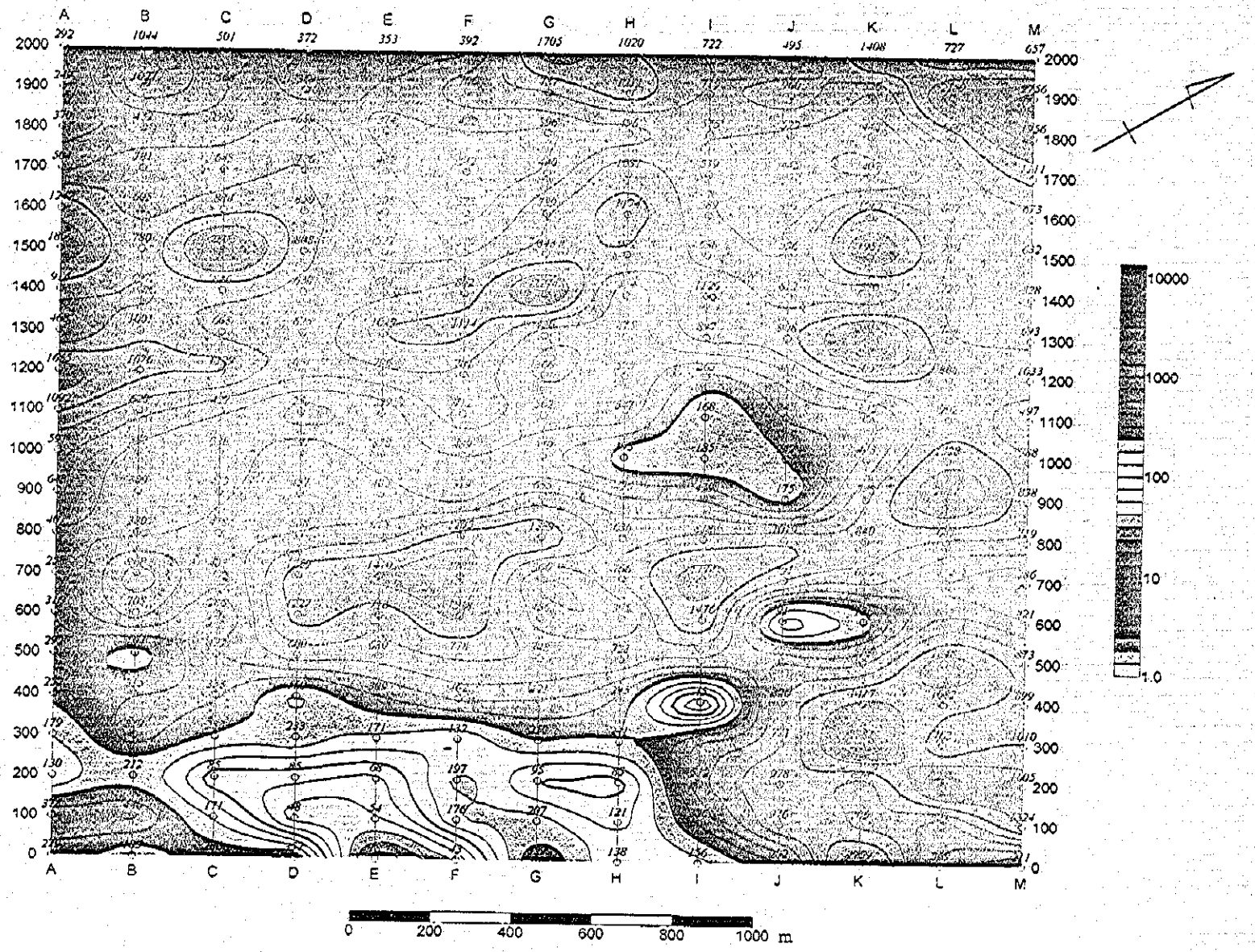

Fig.II-2-8.2 Interpreted resistivity plan map for S.L 400m

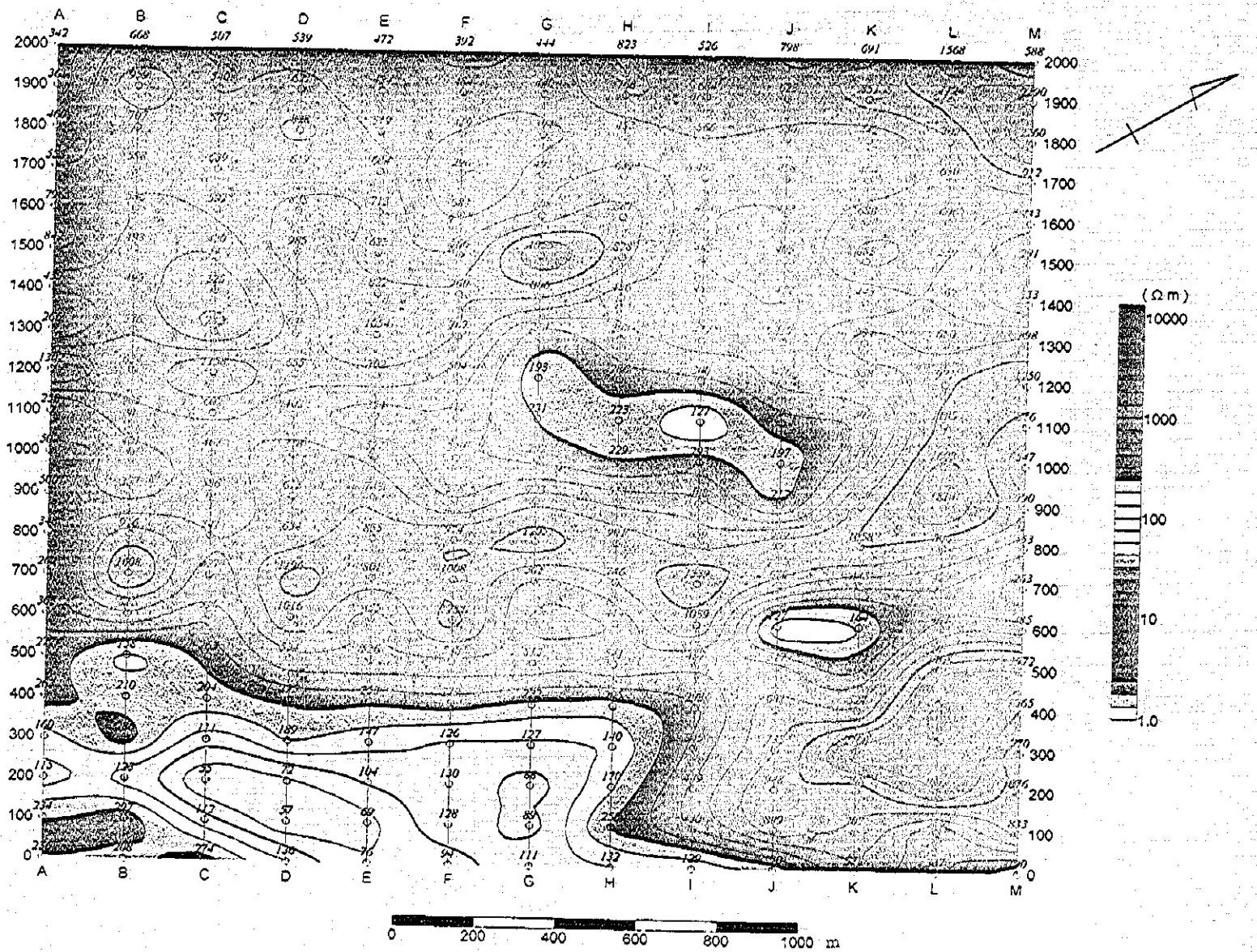

Fig.II-2-8.3 Interpreted resistivity plan map for S.L 300m

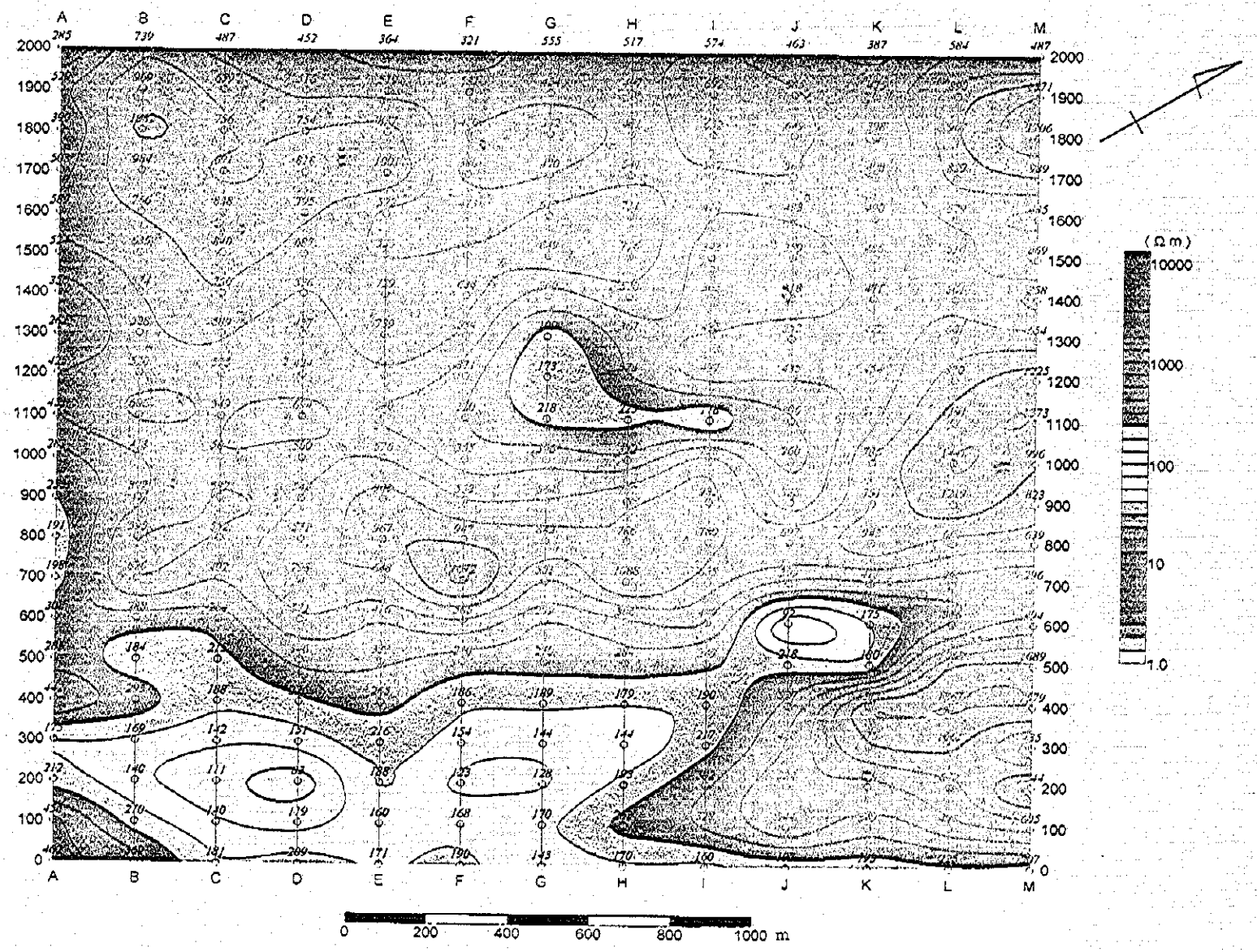

Fig.II-2-8.4 Interpreted resistivity plan map for S.L 200m

The interpreted resistivity plane map of alt.300m is shown in Fig.II-2-8-3. The average interpreted resistivity value is 584.8Ωm (minimum 54.8Ωm, maximum 2900.5Ωm). The low resistivity zone of below 200Ωm is distributed in the south east of survey area, which crosses the survey lines almost perpendicularly in the direction of NE-SW as follows: on the line A between the measurement points 200 and 300, on the line B at the measurement point 100, on the line C between the measurement points 100 and 300, on the line D between the measurement points 0 and 300, on the line E between 0 and 300, on the line F between the measurement points 0 and 300, on the line G between the measurement points 0 and 300, on the line H between the measurement points 0 and 300, on the line I at the measurement point 0. Similarly, the low resistivity zone is assumed connecting each other in the direction of NE-SW as follows: on the line G between the measurement points 1100 and 1200, on the line H between the measurement points 1000 and 1100, on the line I at the measurement point 1100 and on the line J at the measurement point 1000.

The interpreted resistivity plane map of alt.200m is shown in Fig.II-2-8-4. The average interpreted resistivity value is 515.2Ωm (minimum 82.8Ωm, maximum 1705.8Ωm). The low resistivity zone of below 200Ωm is distributed in the south east of survey area, which crosses the survey lines almost perpendicularly in the direction of NE-SW as follows: on the line A at the measurement point 300, on the line B between the measurement points 200 and 500, on the line C between the measurement points 0 and 400, on the line D between the measurement points 100 and 300, on the line E between the measurement points 0 and 200, on the line F between the measurement points 0 and 400, on the line G between the measurement points 0 and 400, on the line H between the measurement points 0 and 400, and on the line I at the measurement point 0. Similarly, the low resistivity zone is distributed on the line I at the measurement point 400, on the line J at the measurement point 600 and on the line K at the measurement point 600. The same as the interpreted resistivity zone distribution of alt 400m, the zone is recognized in the area, which stretches out from the line H at the measurement point 300 to N-S. Another low resistivity zone is assumed from the line G between the measurement point 1100 and 1300 to the line H at the measurement point 1100 and the line I at the measurement point 1100 stretching out to NE-SW.

2-2-3 Result of Laboratory Measurement

The 24 rock samples were collected in the survey area and measured the resistivity in a laboratory, and compared the results with the interpreted resistivity values. The resistivity of each rock sample is shown in Fig.II-2-9, and the results of the comparison are shown in Table II-2-3.

The resistivity of a fresh andesite is between 592 and 3880Ωm, but the altered andesite shows

lower resistivity such as 69Ωm. However, the andesite which is silicified shows more or less higher resistivity as 161Ωm. The resistivity shows a wide range of measurements for that a tuff is between 134 and 723Ωm, the altered tuff shows 98 and 275Ωm and the silicified one turns out to be 123 and 1776Ωm. The resistivity of a slate shows between 297 and 351Ωm (but one of the sample turns out to be 2,043Ωm). The resistivity of a sand stone shows 281 and 569Ωm.

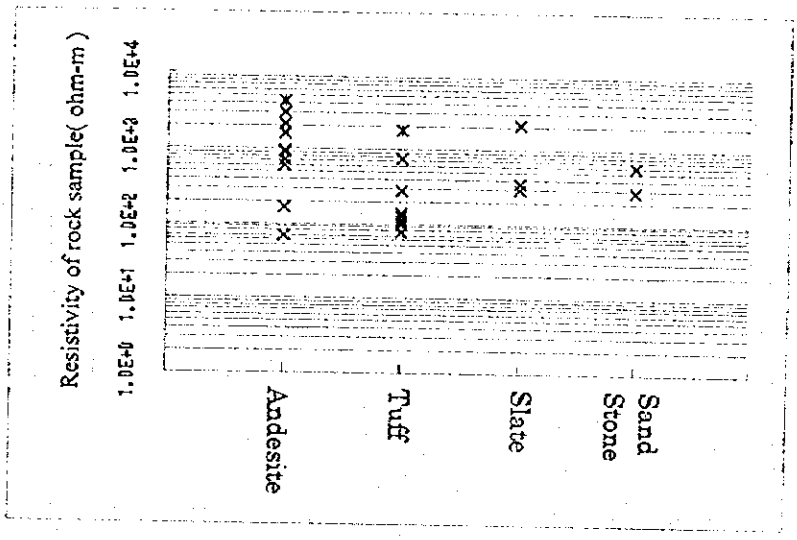

Fig. II-2-9 Resistivity of rock samples

As described above, the resistivity of the rocks collected in the survey area the andesite which is not altered shows the highest resistivity from 600Ωm up to a few thousands Ωm. The resistivity of the tuffs, slates and sand stones are between 150 and 1000Ωm. However, some of the altered rocks show the resistivity below 100Ωm, while some of the silicified rocks show around 2000Ωm

Table II-2-3 Resistivity of rock samples

Sample number	Description	Resistivity (ohm-m)	Sample number	Description	Resistivity (ohm-m)
CR92	andesite	856.7	CR111	tuff	134.5
CR93	andesite	592.4	CR113	tuff (altered)	79.0
CR94	silicified andesite	161.0	CR114	tuff(clay altered)	98.1
CR95	slate	350.4	CR117	silicified tuff	1,775.8
CR96	andesite	944.8	CR119	slate	297.4
CR97	sand stone	281.1	CR120	altered andesite	69.2
CR98	altered tuff	108.6	CR121	slate	2,043.4
CR102	weakly silicified sandy tuff	122.9	CR125	andesite(float)	3,028.2
CR103	slate	351.6	CR127	andesite	2,148.0
CR104	sand stone	569.5	CR128	tuff	723.6
CR105	andesite	3,879.8	GR003	andesite	1,522.6
CR107	andesite	692.1	AR003	altered tuff	274.9

2-3 Considerations

Referring to the resistivity cross section of the survey lines made by conducting two-dimensional interpretation and the resistivity plane map such as for a depth of 50 m from the surface of the earth, alt.400m, alt.300m and alt.200m, the panel diagram of interpreted resistivity plane maps(Fig.II-2-10-1) and the palel diagram of interpreted resistivity cross sections (Fig.II-2-10-2) were illustrated.

The panel diagram of interpreted resistivity plane maps indicates that in the east part of the survey area, the low resistivity zone of below 200Ωm is distributed in the area from the lines A to H, in the width of the measurement points from 0 to 500 in the direction nearly from NE-SW. The panel diagram of interpreted resistivity cross sections shows that the low resistivity anomaly zone indicates a tendency which the resistivity values gradually decrease toward the lines A to E and conversely it gradually increases toward the lines E and H, and toward the lines I and M it turns out to the high resistivity anomaly. Such low resistivity anomaly stretches out from the surface of the earth to a depth of alt.250m. The anomaly section changes the direction on the line H at the measurement point of 400, then stretches out to the line L at the measurement point 600 and connected in lineation (N-S). This anomaly resistivity structure is distributed along the lateral disconinuous resistivity structure which runs toward NE-SW, and NNE-SSW from the line A around the measurement point 500 to the line H around the measurement point 300 that have been assumed by the apparent resistivity plane map and cross section. This structure is considered to be a fault and altered zone run along a fault. The high resistivity anomaly from the lines I to M between the measurement points 0 and 500 which is described above shows the tendency of the resistivity increasing in the direction from the lines I to H and the area too is extending.

Nevertheless, the central and western part of the survey area is mainly the high resistivity zone, the low linear resistivity anomaly of approx.200Ωm is recognized in the area from the line G between the measurement points 1100 and 1200, alt.0m to alt.300m and to the lines I between the measurement points 1000 and 1100, alt.250m to alt.400m. This low resistivity anomaly corresponds with the structure that are assumed by the apparent resistivity plane maps and cross sections that stretch out continuously from the line B around the measurement point 900 to the line K around the measurement point 1000 in the direction from NE-SW to NNE-SSW. It is considered to be the lateral resistivity fault structure. Such as the interpretation conducted in the structure, a strip of the high resistivity zone is distributed from the line B between the measurement points 600 and 900 to the line I between the measurement points 600 to 900. This high resistivity zone, same as the low resistivity zone described earlier, changes the direction from the line I to N-S, and then stretches out to the line M between the measurement points 1000 and 1200.

Apart from these structures, the apparent resistivity plane maps and cross sections shows that in the south west of the survey area, the structure in the direction of NE-SW to NNE-SSW from the line A

at the measurement points 1800 to the line E at the measurement point 1800, and the structure which stretches out to the line C at the measurement point 0 from the line A at the measurement point 200, and also from the line M at the measurement point 100 to the line L at the measurement point 0 are all assumed.

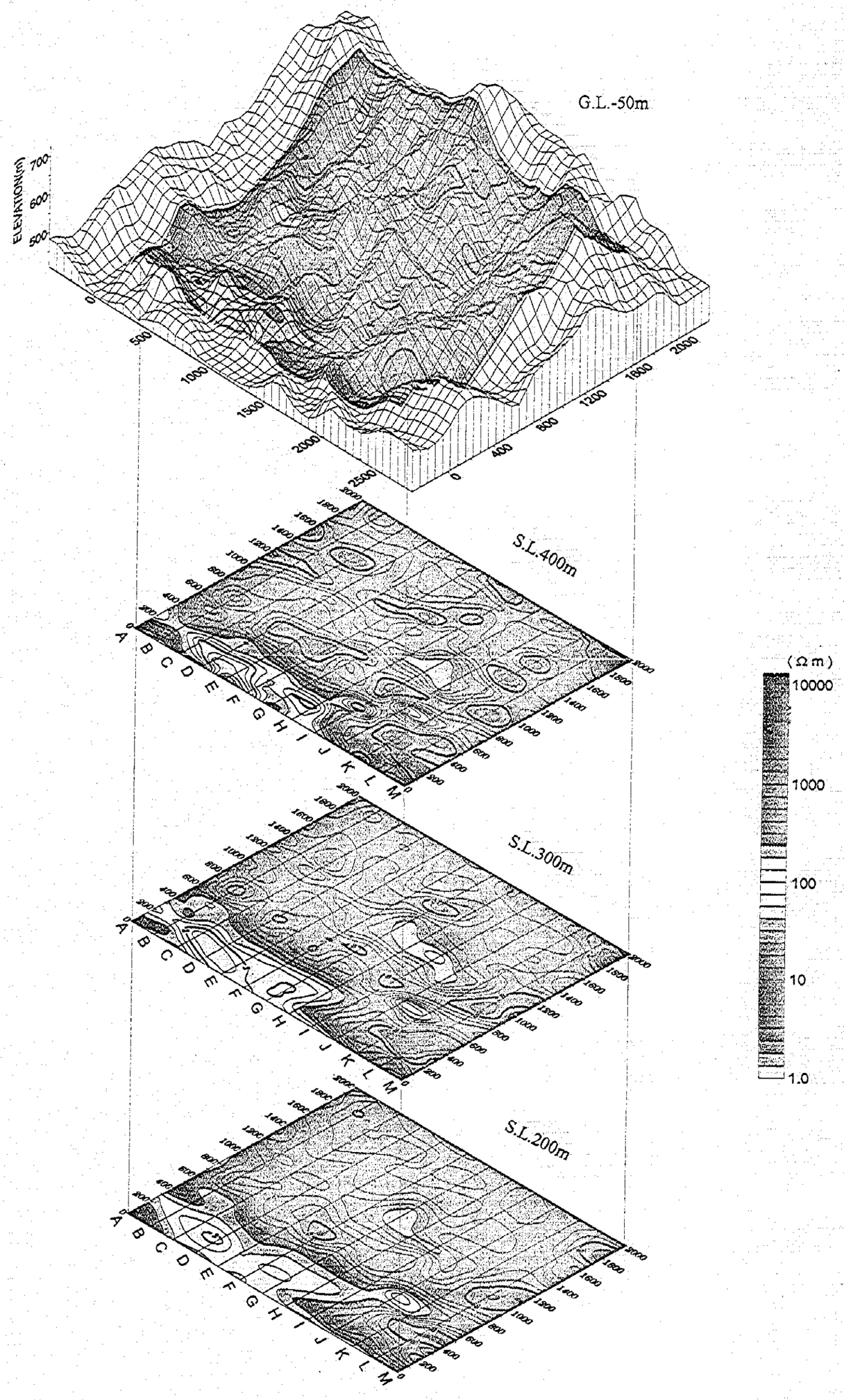

Fig.II-2-10.1 Panel diagram of interpreted resistivity plan maps

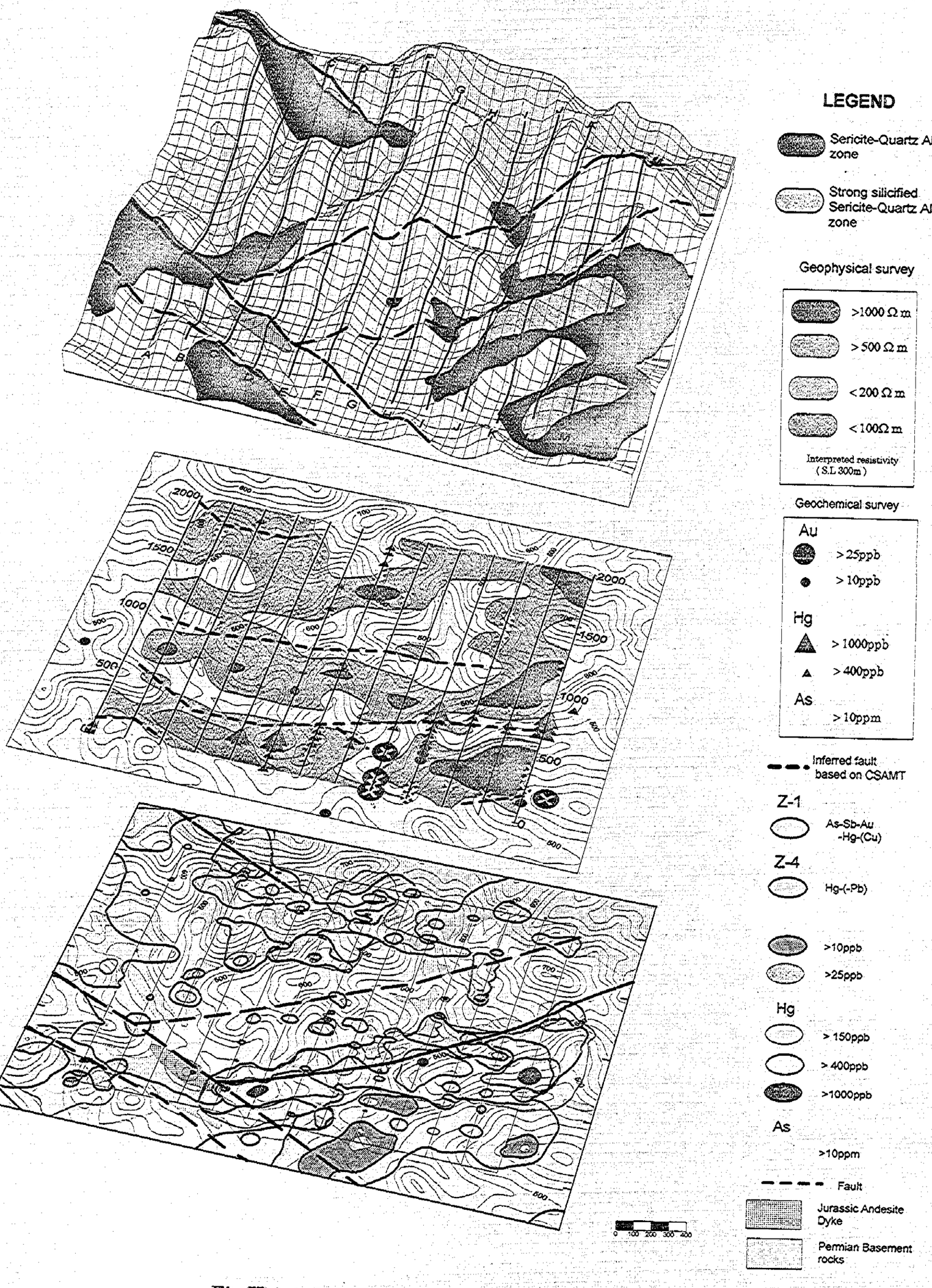

Fig.II-3-1 Interpretation Map of the Survey

CHAPTER 3 COMPRIHENSIVE ANALYSIS OF SURVEY RESULTS

The interpretation map of the survey is shown in Fig. II-3-1.

The area west of the anomalous zone of low resistivity which continues from point 500m on Line A to point 500m on Line H, and the anomalous zone of low resistivity changing direction from Line H and continuing to Line M is for the most part a zone of high resistivity. In these areas Permian basement rock occurs at a shallow depth, and the area of high resistivity corresponds to the resistivity values for shale or sandstone.

In the eastern part including the above-mentioned zones of low resistivity, tuffaceous rocks of Permo-Triassic age are distributed; these have undergone wide-ranging argillization accompanied by silicification, and the low resistivity is considered to correspond to the altered tuff.

In this area geochemical anomalies in Au, As, Sb and Hg, suggesting gold mineralization, are spread out overlapping the alteration zone. The distribution of the above-mentioned geochemical anomalities does not accompany the anomalous zone of low resistivity which continues from point 500m on Line A to point 300m on Line H, but from Line A to near Line E an anomal zone was observed further to the southeast. An anomal zone in Au, Sb and As is located on the eastern side of the resistivity discontinuous line in a N-S direction which continues from point 400m on Line H to point 600m on Line L. In contrast to this, an anomal zone in Hg and As showing a higher halo of mineralization matches the low resistivity zone on the west side of this discontinuous line and an anomal zone also spreads out on the eastern side, partially straddling the discontinuous line of the NE-SW direction.

In the anomal zone in Au, Sb and As, low resistivity occurs in the surface area, and a high resistivity zone was observed at a depth of 100m to 250m underground in the vertical distribution of resistivity. This high resistivity zone has a resistivity value close to that of andesite in laboratory tests, but in view of the geological conditions there is a strong possibility of the existence of silicified tuff or a silicification zone.

In consideration of the fact that the homogenization temperature of fluid inclusion of quartz at the surface is low, at 150℃, it is anticipated that there is gold mineralization accompanying this underground high resistivity zone. The anomal zone in Au, Sb and As, obtained from the geochemical survey, stretching to the south from the detailed survey zone, has the same kind of geological condition and alteration type, and in the lower part of the high anomalies in Au which occur there it is anticipated that the same kind of silicified zone is present.

On the other hand, the anomal zone in Hg and As matches the zone of low resistivity along the high resistivity zone of basement rocks on the western side of the resistivity discontinuous line in a N-S direction, between Line H and Line M. This low resistivity zone continues in slab form to a depth below sea level. If the anomal area in Hg and As is considered to represent a mineralization

halo in the upper part of hydrothermal deposits, the presence of gold mineralization may be anticipated deep underground. Also, the resistivity structure in the lower part of the anomal zone in Hg and As occurring from Line E to Line G, differing from that between Line H and Line M, is spread over a width of 200m and a depth of close to 200m in depth, and geochemical anomalies occur close to the border area between this low resistivity zone and the high resistivity zone located in the west of the low resistivity zone.

Of the prospective area inferred from the geochemical survey, in the shallow prospects the silicification zine either occurs at a comparatively shallow depth or is already exposed, and from the results of the geophysical survey the silicification zone continues from the surface to a depth of 200m or close to 250m. In the deeper prospects, from Line H to Line M a low resistivity zone continues to a depth of 350m-400m, and at the deeper part and towards Line M the resistivity gradually rises. No high resistivity zone clearly indicating quartz veins/silicified zones was observed, but the presence of gold mineralization is anticipated in the deeper part of the low resistivity zone and in the zone of comparatively high resistivity on Lines L and M. This depth is estimated to be close to sea level. The results of the geochemical survey made the geochemical anomal zone in Hg and As from Line E to Line G a deep prospective site (D-B). However, according to the results of the geophysical survey, the resistivity structure of this lower part was the northern edge of a fusiform zone of low resistivity 200m deep and 200m wide, and was different to the low resistivity zone from Line H to Line M. The depth of gold mineralization here is thought to be close to 300m, the depth at which the resistivity value rises.

The resistivity discontinuous line from Line A to close to the end of Line D which is in high resistivity zone in the distribution area of basement rocks accompanies the distribution of geochemical anomalies in As and weak anomalies in Hg, and also matches a zone of sericite-quartz alteration zone. Boiling phenomenon was observed in the quartz veins near here, and there is a strong possibility of the existense of gold mineralization within the basement rocks.

Close to the detailed survey zone, alteration, geochemical anomalies and resistivity structure are regulated by the N-S and NE-SW faults, and from the results of the survey it was observed that there was a tendency for the faults and fractures in the N-S direction in particular to have a strong involvement.

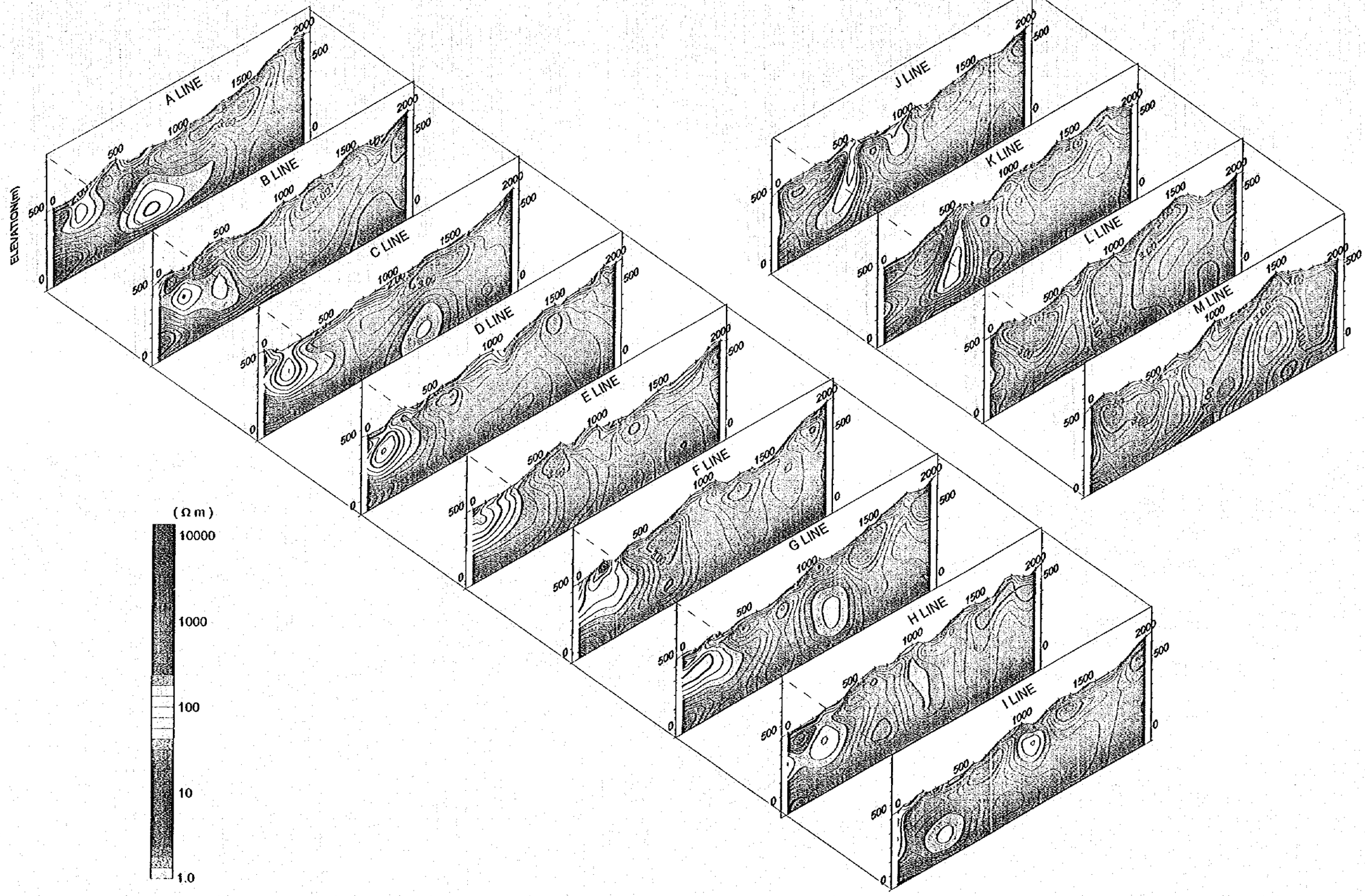

Fig.II-2-10.2 Panel diagram of interpreted resistivity cross sections

PART Ⅲ CONCLUSION AND RECOMMENDATION

CHAPTER 1 CONCLUSION

The Upper Huai Nam Sala area is made up of Permian sedimentary rocks, the basement of this area, Permo-Triassic rhyolitic volcanic rocks, Permo-Triassic andesitic volcanic rocks, Jurassic intrusive rocks and Quaternary riverbed deposits. The basement rocks of Permian age are distributed in the western part of the detailed survey zone.

Within this area, two fault systems were observed, a N-S fault and a NE-SW fault. Both fault systems have a vertical displacement, with the western or northwestern block relatively raised. The NE-SW fault is developed on the synclinal axis of the Permian rocks, and continues to the southwestern part of the Survey Area. The N-S fault converges with the NE-SW fault, and is thought to be derived from this fault.

The alteration zones and mineral occurrences are regulated by this fault system and are developed in Permo-Triassic tuff as host rocks. The alteration zones are zones of argillization accompanied by silicification, and while there is some difference in the strength of silicification, the alteration zones are classified into weakly acidic to neutral alteration zone, that is, sericite+quartz zone; sericite+kaolinite ± quartz zone; sericite+montmorillonite ± kaolinite ± quartz zone; montmorillonite±kaolinite zone; weak or no alteration zone and display a zonal structure. The mineral occurrences are the area where quartz veins are accompanied by these alteration zones or strongly silicified altered rocks. The strongest alteration zone spread along the NE-SW fault on the south side of the detailed zone. It is made up mainly of sericite+quartz zone accompanied by strong silicification, and here in the assey analysis, values of Au=5.6g/t, 1.0g/t were obtained.

The alteration zone which is distributed from Line F to the starting point - 1000m point on Line M is observed to have a zonal structure, with a central zone of sericite+quartz followed by a sericite+kaolinite ± quartz zone and a sericite+montmorillonite ± kaolinite ± quartz zone. Overlapping this alteration zone, geochemical anomalies in Au, As, Sb and Hg, suggesting the stongest gold mineralization, are observed in the whole of the Survey Area. In the geophysical survey, this corresponds to the border area between the high resistivity zone in the western part of the detailed survey zone and the low resistivity zone on the eastern side. Anomalous values in Au, As and Sb are distributed from Line J to the starting point - 500m point on Line M; in the surface area there occurs a low resistivity zone and at a depth of 100m-300m a high resistivity zone which thought to be a silicification zone; and it is anticipated the occurrence of gold. An anomaly zone of Hg and As, suggesting the mineralization halo of the upper part of hydrothermal deposits, occurs from Line E to Line M along the resistivity discontinuous line(the border area between basement rock and tuff) of the geophysical survey. From Line E to Line I and from Line J to Line M there is a difference in the structure of resistivity in the lower part, but gold mineral prospects are expected where a low resistivity zone shifts to a high resistivity zone.

Also, anomalous values in Au, As and Hg continue southwards from the starting point of Line I, and in this area also the existence of a silicified zone accompanied by gold mineralization is anticipated.

Since the boiling phenomenon is observed and the homogenization temperature of fluid inclusion near the surface seems to be low, at 150℃, there is a very strong possibiility indeed that the center of the gold mineralization effect is still further down, and that deep down there is a quartz vein and silicified zone accompanied by gold.

CHAPTER 2 RECOMMENDATION FOR THE THIRD PHASE SURVEY

There is a strong possibility of the presence of gold mineral prospects in the lower part of the anomaly zone in Hg and As along the resistivity discontinuous line and the high resistivity zone accompanying the comparatively shallow zone of anomaly in Au, As and Sb extracted in the Survey this year. Next year it is desirable that a survey be made of the mineralization condition and of alteration through a drilling survey in the lower parts of each anomaly zone, and the presence or otherwise of gold mineral prospects be confirmed.

REFERENCES

Goldstein,M.A.and Strangway,D.W., 1975: Audio-frequency magnetotellurics with a grounded electric dipole source. Geophysics, 40, 669-683.

Govett,G.J.S., 1983: Handbook of exploration geochemistry, Volume 2. Statistic and data Analysis in Geochemical Prospecting. ELSEVIER SCIENTIFIC PUBLISHING COMPANY, 437p.

Harmon, R.S. et al.,1984: Regional O-,Sr- and Pb isotope relationships in late Cenozoic calk-alkaline lavas of the Andean Cordillera. J. Geol. Soc. Lond., 141, 803-822.

JICA and MMAJ, 1995: Report on the cooperative mineral exploration in the Chiang Khong, Doi Chong, Ratchaburi Area, the Kingdom of Thailand, phase I. Japan International Agency and Metal Mining Agency of Japan

Kuno,H.,1966:Lateral variation of basalt magma type across continental margins and island arcs. Bull.Volcanol., 29, 195-222.

Lepeltier, C., 1969: A simplified statistical treatment of geochemical data by graphical representation. Econ. Geol.,64,538-550.

Meschede,M.,1986: A method of discriminating between different types of mid-ocean ridge basalts and continental tholeiites with the Nb-Zr-Y diagram. Chem. Geol. 56, 207-218.

Nabighian,Misac N.,1992:Electromagnetic methods. Applied Geophysics, Volume 2, Part B, 713-809.

Miyashiro,A.,1974: Volcanic rock series in island arcs and active continental margins. Am.J.Sci., 274,321-355.

Mullen,E.D.,1983: MnO/TiO2/P2O5: a minor element discriminant for basaltic rocks of oceanic environments and its implications for petrogenesis. Earth Planet Sci. Lett., 62, 53-62.

Pearce,J.A. and Cann,J.R.,1973: Tectonic setting of basic volcanic rocks determined using trace element analysis. Earth Planet Sci. Lett., 19,290-300.

Sinclair,A.J., 1976: Application of probability graphs in mineral exploration. Special volume No.4,

The Association of Exploration Geochemists.

Steiger,R. and Jaeger,E.,1977:Subcommision on geochronology, Comvention on the use of decay constants in geo- and cosmo-chronology.Earth Planet. Sci. Lett., 36, 359-362.